Semiconductor Physics, Quantum Electronics & Optoelectronics, 2017. V. 20, N 4. P. 475-480.
doi: https://doi.org/10.15407/spqeo20.04.475

PACS 73.50.Pz, 81.05.Rm

Photoconductivity relaxation and electron transport in macroporous silicon structures

L.A. Karachevtseva, V.F. Onyshchenko, A.V. Sachenko
V. Lashkaryov Institute of Semiconductor Physics,
National Academy of Sciences of Ukraine
41, prospect Nauky, 03680 Kyiv, Ukraine,
e-mail: lakar@isp.kiev.ua

Abstract. Kinetics and temperature dependence of photoconductivity were measured in macroporous silicon at 80…300 K after light illumination with the wavelength 0.9 μm. The influence of mechanisms of the charge carrier transport through the macropore surface barrier on the kinetics of photoconductivity at various temperatures was investigated. The kinetics of photoconductivity distribution in macroporous silicon and Si substrate has been calculated using the finite-difference time-domain method. The maximum of photoconductivity has been found both in the layer of macroporous silicon and in the monocrystalline substrate. The kinetics of photoconductivity distribution in macroporous silicon showed rapid relaxation of the photoconductivity maximum in the layer of macroporous silicon and slow relaxation of it in the monocrystalline substrate.

Keywords: photoconductivity kinetics, macroporous silicon, distribution of charge carriers..

Manuscript received 14.09.17; revised version received 17.10.17; accepted for publication 07.12.17; published online 07.12.17.

1. Introduction

Porous silicon has found application in sensors, receivers, in integrated microchips. Efficient conductivity and photoconductivity in macroporous silicon decrease with increasing the concentration and volume fraction of macropores [1]. Reducing the thickness of the space charge region (SCR) at small macropore diameters was evaluated, too [1]. The effective lifetime of photocarriers in absorbers based on macroporous thin films decreases due to recombination at large areas of the pore surface [2]. The effective carrier lifetime of surface-passivated macroporous silicon [2, 3] and black silicon with cones and pyramids [4] is dependent on the surface morphology and passivation, bulk lifetime. Gas [5, 6] and biological sensors [7] are developed on the porous silicon with CMOS-compatible manufacturing. Macroporous silicon [8, 9] and black silicon nano-textured by cones and pyramids [4] are used as solar cells.

The possibilities to enhance the properties of nanostructured surfaces were demonstrated on the "polymer-multiwall carbon nanotube" composites and their nanocoatings on macroporous silicon structures [10]. The photoluminescence quantum yield in CdS nanocrystals on the surface of oxidized macroporous silicon with the optimum thickness of SiO_2 layer increases with time up to 28%, which is higher than that in CdS quantum dots [11]. The photoluminescence of polyethyleneimine with carbon multiwall nanotubes on macroporous silicon with a microporous layer is about six times higher intense than that on monocrystalline silicon, macroporous silicon and oxidized macroporous silicon [12, 13].

The distribution of excess minority carrier concentration in macroporous silicon was calculated in [14] at the spatially homogeneous generation of charge-carriers. This value decreases sharply with the depth of macropores lower than 10 μm and not changes for the macropore depth 100…200 μm [14]. The numerical calculation of the distribution of excess minority carrier concentration in macroporous silicon on Si substrate has been performed in [15] at light illumination with the wavelengths 0.95, 1.05 and 1.1 μm. It was shown that there are two maxima in the distribution of photocarriers at the wavelength 0.95 μm. The first maximum of photohole distribution in macroporous silicon is in the macroporous layer, the second one lies in the monocrystalline substrate [15].

Macroporous silicon layers are used as antireflective coatings for silicon solar cells [16, 17]. Penetration of light into the pores and its multiple reflections from the pore walls increases absorption of light. The scattering of light leads to an increase in the optical path, and consequently, to an increase in the absorption of light [18]. If the pores are etched on the two silicon surfaces, then multiple reflection of light between these surfaces is realized due to availability of angles higher than the critical angle of the total internal reflection [19].

The aim of this work was the experimental and theoretical study of the relaxation time of photoconductivity in macroporous silicon and silicon substrate at different temperatures. The influence of mechanisms of the charge carrier transport through the macropore surface barrier on the kinetics of photoconductivity was also investigated.

2. Measurement of the photoconductivity kinetics at different temperatures

Relaxation of photoconductivity was measured in the samples of *n*-type macroporous silicon structures (Fig. 1) and monocrystalline silicon with the equilibrium electron concentration $n_0 = 10^{21}$ m^{-3}, the [100] orientation was used. The samples of macroporous silicon were fabricated by electrochemical etching of monocrystalline silicon under illumination from the back side [13]. The average pore diameter was 2 μm, the average distance between pores was 2 μm. The sample thickness was 500±10 μm, the depth of pores was 100…150 μm. The samples were illuminated using the GaAs laser diode with the wavelength 0.9 μm. The pulse duration was 40 ns. The intensity of the laser pulse was 23 W/m^2. Numerical calculations were carried out by the finite-difference time-domain method [20] to determine the kinetics of distribution of the conductivity in macroporous silicon.

Fig. 2 shows the experimental dependencies of photoconductivity relaxation for the sample of macroporous silicon on the monocrystalline silicon substrate measured at different temperatures. It is evident from Fig. 2 the large non-exponential part of photoconductivity relaxation.

The photoconductivity relaxation time (Fig. 3) in macroporous silicon is hundreds of microseconds at room temperature and tens of milliseconds at temperatures below 200 K, which is twice the photoconductivity relaxation time in monocrystalline silicon due to some peculiarities of photoconductivity in macroporous silicon.

Macroporous silicon has a large surface of macropores $(3…5)\cdot10^3$ cm^2/cm^3 with depleted surface potential (Fig. 4). The dimensionless surface potential in darkness is about 12 at room temperature and corresponds to 0.31 eV [21]. Light-generated electron-hole pairs diffuse into the spatial charge region on the macropore surface (Fig. 4), which is a potential well for minority charge carriers and a potential barrier for majority charge carriers. Excess charge carriers are drifting in an electric field near the surface of the pores and are separated. The separated charge carriers create a concentration gradient of excess charges (diffusion to balance the drift of carriers). As a result, charge carriers are accumulated on the surface, diminish the surface electrostatic field and change the surface level charge. All these effects change the photoconductivity relaxation time. The accumulated charge on the surface of the macropores changes the conductivity of the macroporous layer in the direction along macropores.

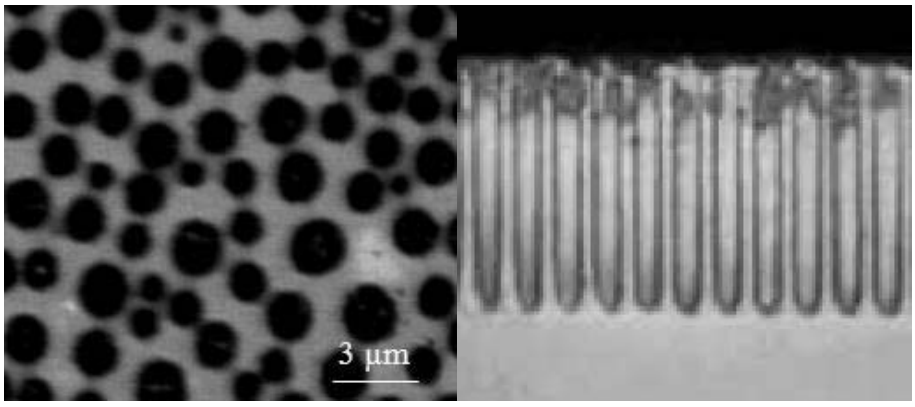

Fig. 1. Image of macroporous silicon.

Semiconductor Physics, Quantum Electronics & Optoelectronics, 2017. V. 20, N 4. P. 475-480.
doi: https://doi.org/10.15407/spqeo20.04.475

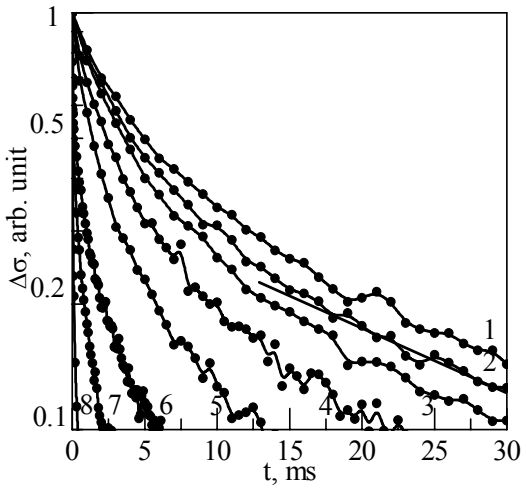

Fig. 2. Experimental dependences of the photoconductivity relaxation of macroporous silicon at temperatures *T*, K: *1* – 80; *2* – 100; *3* – 120; *4* – 160; *5* – 180; *6* – 200; *7* – 260; *8* – 300.

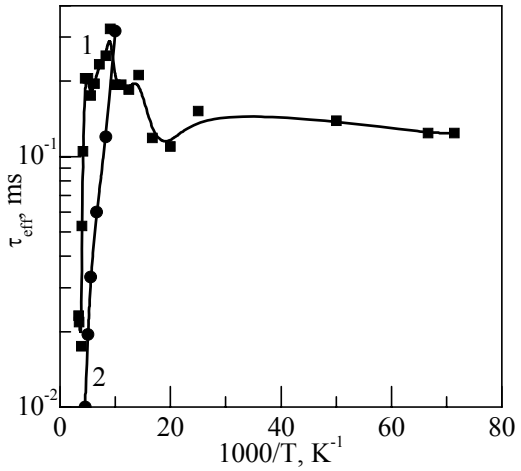

Fig. 3. Temperature dependences of photoconductivity relaxation time in macroporous silicon (curve *1*) and in monocrystalline silicon (curve *2*).

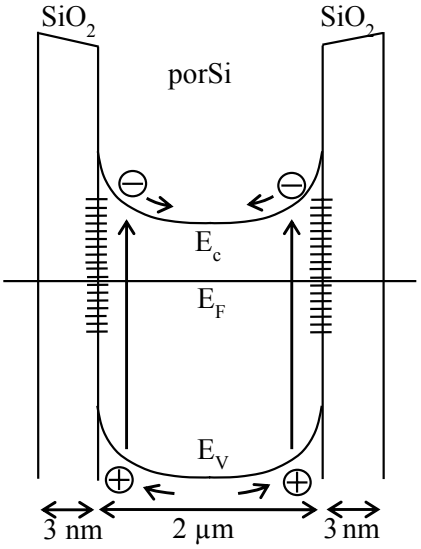

Fig. 4. Scheme of energy zones on the surfaces of silicon bordering with two pores.

3. Numerical calculation of the distribution kinetics of the specific photoconductivity over the thickness of macroporous silicon

The minority carrier time-dependent diffusion equation for macroporous *n*-silicon (one-dimensional case in the *x*-direction parallel to the macropore) is:

$$\frac{\partial}{\partial t}\delta p(x,t) = D_p \frac{\partial^2}{\partial x^2}\delta p(x,t) - \frac{\delta p(x,t)}{\tau_{eff}} \ , \qquad (1)$$

here: $\delta p(x)$ is the distribution function of the excess minority carrier concentration in the *x*-direction, τ_{eff} – effective recombination time of excess minority carriers in the layer of macroporous silicon [3, 14, 15], D_p – diffusion coefficient of minority carriers.

The minority carrier diffusion equation for above conditions is:

$$D_p \frac{\partial^2}{\partial x^2}\delta p(x) - \frac{\delta p(x)}{\tau_{eff}} + g_{0p}(\alpha)\exp(-\alpha x) = 0 \ , \qquad (2)$$

where α is the absorption coefficient of silicon, $g_{0p}(\alpha)$ – generation rate of excess minority charge carriers at the illuminated surface.

The boundary conditions for macroporous silicon on silicon substrate are:

$$\frac{dp_1}{dx}(0,t) = s_1 p_1(0,t) \ , \qquad (3)$$

$$\frac{dp_2}{dx}(h,t) = s_2 p_2(h,t) \ , \qquad (4)$$

$$(1-P)D\frac{dp_1}{dx}(h_1,t) = D\frac{dp_2}{dx}(h_1,t) - Ps_{por}p_2(h_1,t) \ , \qquad (5)$$

$$p_1(h_1,t) = p_2(h_1,t) \ , \qquad (6)$$

where: $p_1(x, t)$ is the distribution function of the excess minority carriers in the macroporous layer at the time *t*, $p_2(x, t)$ – distribution function of the excess minority carriers in the monocrystalline silicon substrate at the time *t*. The system of equations (1)–(6) was solved numerically by the finite-difference time-domain method [20]. We obtained the distribution of excess minority carriers in macroporous silicon through the five-second time interval. The electromagnetic wave is incident on the surface of macroporous silicon along the normal to the macropores. The kinetics of the specific photoconductivity in the direction perpendicular to macropores is defined as follows:

$$\delta\sigma_{\perp}(x,t) = e\left(\mu_n + \mu_p\right)\begin{cases}\dfrac{1-P}{1+P}\delta p_1(x,t), & 0 < x < h_1 \\ \delta p_2(x,t), & h_1 < x < h \ . \end{cases} \qquad (7)$$

Semiconductor Physics, Quantum Electronics & Optoelectronics, 2017. V. 20, N 4. P. 475-480.
doi: https://doi.org/10.15407/spqeo20.04.475

The kinetics of the averaged specific photoconductivity in macroporous silicon in the direction perpendicular to the pores is defined by the integral:

$$\delta\sigma_{\perp}(t) = \frac{1}{h}\int_0^h \delta\sigma(x,t)dx =$$

$$= \frac{e(\mu_n+\mu_p)}{h}\left(\frac{1-P}{1+P}\int_0^{h1}\delta p_1(x,t)dx + \int_{h1}^{h}\delta p_2(x,t)dx\right). \quad (8)$$

The kinetics of the specific photoconductivity in the direction parallel to the macropores is defined as follows:

$$\delta\sigma_x(x,t) = e\left(\mu_n+\mu_p\right)\begin{vmatrix}(1-P)\delta p_1(x,t), & 0<x<h_1\\ \delta p_2(x,t), & h_1<x<h.\end{vmatrix} \quad (9)$$

The kinetics of the averaged specific photoconductivity in macroporous silicon in the direction parallel to the pores is determined by the integral:

$$\delta\sigma_x^{-1}(t) = \frac{1}{h}\int_0^h \frac{dx}{\delta\sigma(x,t)} =$$

$$= \frac{1}{he(\mu_n+\mu_p)}\left((1-P)\int_0^{h1}\frac{dx}{\delta p_1(x,t)} + \int_{h1}^{h}\frac{dx}{\delta p_2(x,t)}\right). \quad (10)$$

Fig. 5 shows the normalized distribution of the specific photoconductivity in the macroporous silicon. Electromagnetic waves with the wavelength 0.9 μm were incident on macroporous silicon in the direction parallel to the pores. The bulk lifetime of monocrystalline silicon was equal to 10 μs. The upper curve *1* corresponds to the initial distribution of the specific photoconductivity calculated according to the formulas (2) to (6). Curves *2* to *5* correspond to the distribution of the specific photoconductivity with variation of the concentration of excess minority carriers with the time interval 5 μs. The normalized distribution of the specific photoconductivity in macroporous silicon structure has two maxima corresponding to the electromagnetic wave with the wavelength 0.9 μm is incident on the structure as in [15]. These maxima are related with: (1) absorption of electromagnetic wave of this length, (2) presence of macropores and (3) diffusion of excess charge carriers.

The electromagnetic waves incident on the monocrystalline substrate through the bottom of macropores create an additional maximum of distribution of specific photoconductivity near the bottom of macropores. Two maxima are separated by a minimum caused by the decrease of a generation of excess charge carriers as a result of absorption and diffusion along macropores. The conductivity in the formula (7) of monocrystalline silicon between macropores is multiplied by the factor $(1-P)/(1+P)$ according to the theory of effective medium. That leads to a sharp decrease in the photoconductivity function at the boundary between macroporous layer and monocrystalline substrate (Fig. 5, curve *1*). There is no such discontinuity or a sharp decrease in the distribution of concentration of excess charge carriers (Fig. 5, curves *2* to *5*), because the boundary condition (6) requires the equality of concentration at the boundary between macroporous layer with monocrystalline substrate. Fig. 6 shows dependences of the normalized specific photoconductivity on time in macroporous silicon (curves *1*, *2*), on boundary macroporous silicon-Si substrate (curve *3*) and in a monocrystalline Si substrate (curve *4*). The kinetics of the conductivity distribution in macroporous silicon showed a rapid relaxation of the photoconductivity maximum in the layer of macroporous silicon (curve *1*), and slow relaxation of the photoconductivity maximum in the monocrystalline substrate (curve *4*).

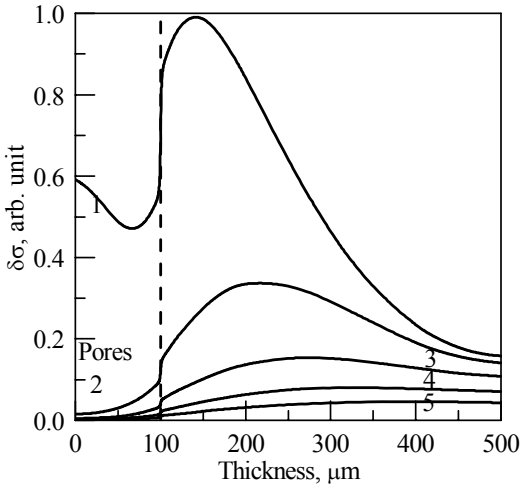

Fig. 5. Normalized distribution of specific photoconductivity in macroporous silicon with the time interval, μs: *1* – 0, *2* – 5, *3* – 10, *4* – 15, *5* – 20. Depth of pore is 100 μm.

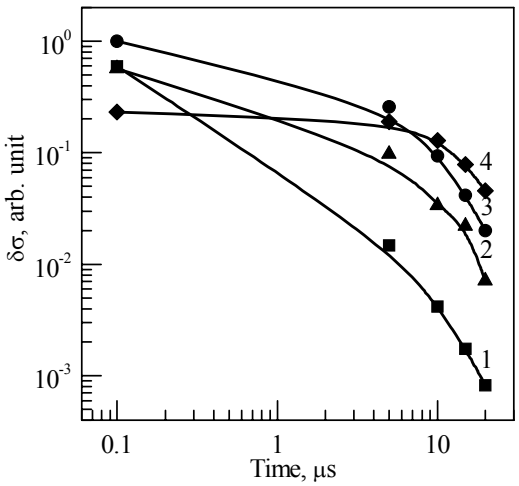

Fig. 6. Dependence of the normalized specific photoconductivity on a time in macroporous silicon and in the monocrystalline Si substrate, μm: *1* – 0, *2* – 100, *3* – 140, *4* – 400.

Semiconductor Physics, Quantum Electronics & Optoelectronics, 2017. V. 20, N 4. P. 475-480.
doi: https://doi.org/10.15407/spqeo20.04.475

4. Transport-recombination processes at the macropore surface

The photoconductivity on the macropore surface is defined by the excess electrons, which fill the equilibrium Schottky layer [21]. The kinetic equation for photoconductivity relaxation is as follows:

$$\frac{d\Delta N(t)}{dt} = -j_r(t) = -\frac{J_s}{e}\left(\exp\left(\frac{\Delta Y(t)}{\beta}\right)-1\right). \qquad (11)$$

Here, $\Delta N(t)$ is the surface excess electron concentration, $j_r(t)$ – recombination current (the recombination flow from volume to surface through the surface barrier), J_s – surface density of the saturated current. The change in the dimensionless potential $\Delta Y(t)$ with the electromagnetic wave intensity falling on the macropore surface is equivalent to the change in the dimensionless potential at forward bias. In this case, there are three main transport-recombination processes: over-barrier transfer, quantum-mechanical tunneling through the barrier to the recombination centers, and recombination in the spatial charge region. These processes are characterized by the coefficient β. Solving the equation (11) by using the initial conditions [21], we obtain for the case $\Delta Y(t) > 1$:

$$\Delta N(t) \approx$$
$$\approx 2L_{Dn}n_0\left(\sqrt{Y_0} - \sqrt{Y_0 - \Delta Y(t=0) + \beta\ln\left[1 + t/\tau_r(\beta)\right]}\right). \qquad (12)$$

Here is: $\tau_r(\beta) = \dfrac{e\beta n_0 L_{Dn}}{J_s\sqrt{Y_0}}\exp\left(-\dfrac{\Delta Y(t=0)}{\beta}\right)$. The equation (12) is normalized by the maximum value, and we introduce an effective photoconductivity relaxation time τ_{eff}, as a decrease in the photoconductivity by half. Under these conditions, we obtain an equation that connects the values $\Delta Y(t=0)$, β, τ_{eff}:

$$\frac{\Delta N_{nor}(t=\tau_{eff})}{2} =$$
$$= \frac{\sqrt{Y_0} - \sqrt{Y_0 - \Delta Y(t=0) + \beta\ln\left[1+\tau_{eff}/\tau_r(\beta)\right]}}{\sqrt{Y_0} - \sqrt{Y_0 - \Delta Y(t=0)}} = \frac{1}{2}. \qquad (13)$$

Here, the value $\Delta Y(t=0)$ depends on the intensity of the electromagnetic radiation, β indicates domination of the transport-recombination process, and τ_{eff} characterizes the kinetics of recombination.

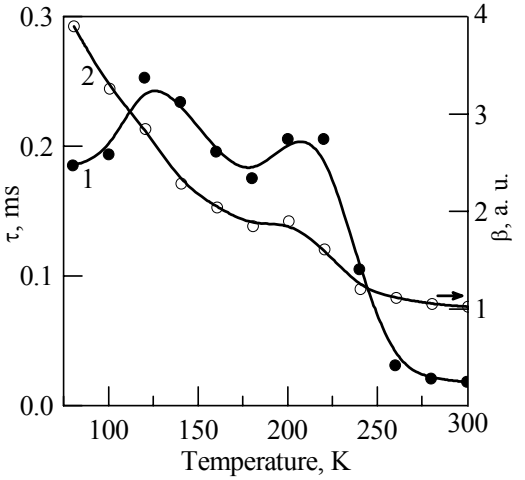

Fig. 7. The temperature dependence of the effective photoconductivity relaxation time (curve *1*) and the coefficient β (curve *2*) in macroporous silicon.

Fig. 7 shows the temperature dependence of the effective photoconductivity relaxation time (curve *1*) and the coefficient β determined using the formula (13) (curve *2*) in macroporous silicon on the monocrystalline silicon substrate. According to Fig. 7, a region with the coefficient $\beta \approx 1$ is realized in the temperature range from 240 up to 300 K, which is typical for the thermionic emission mechanism of recombination. In this temperature range, the effective relaxation time of photoconductivity does not change. The temperature dependence of the effective relaxation time of photoconductivity at 220…260 K increases sharply and has an activation character with the energy 0.31 eV. It is almost independent of temperature below 220 K. And in the temperature range from 140 up to 200 K, a region with the coefficient β close to 2 is realized, which indicates the dominance of the generation-recombination mechanism. When the temperature is lower than 140 K, the coefficient β begins to sharply increase, which indicates the dominance of the tunnel mechanism.

Strong relative change of relaxation time (Fig. 7, curve *1*) and the coefficient β (Fig. 7, curve *2*) is observed at $T < 140$ K with the tunnel mechanism of the excess electron recombination and at $T > 240$ K with the thermionic emission mechanism of electron recombination process. The coefficient β of the generation-recombination mechanism in the spatial charge region (curve *2*) correlates with the temperature dependence of relaxation time (curve *1*).

5. Conclusions

The influence of current transport mechanisms through the macropore surface barrier on the photoconductivity kinetics are investigated experimentally and theoretically in macroporous silicon and silicon substrate at various temperatures. The photoconductivity maxima are revealed both in the layer of macroporous silicon and in the monocrystalline substrate.

The conductivity kinetic distribution in macroporous silicon and silicon substrate showed a rapid relaxation of the photoconductivity maximum in the layer of macroporous silicon and slow relaxation of the photoconductivity maximum in monocrystalline silicon. Diffusion, surface potential, accumulation of charge on the surface and surface levels slow down relaxation of non-equilibrium charge carriers on the surface of pores.

Strong relative change of relaxation time and the coefficient β is observed for tunnel mechanism of the excess electron recombination and for the thermionic emission mechanism of electron recombination process. The coefficient β of the generation-recombination mechanism in the spatial charge region correlates with temperature dependence of relaxation time.

References

1. Onyshchenko V.F., Karachevtseva L.A. Conductivity and photoconductivity of two-dimensional macroporous silicon structures. *Ukr. J. Phys*. 2013. **58**, No. 9. P. 846–852.
2. Ernst M., Brendel R. Modeling effective carrier lifetimes of passivated macroporous silicon layers. *Sol. Energy Mater. Sol. Cells*. 2011. **95**, No. 4. P. 1197–1202.
3. Onyshchenko V.F., Karachevtseva L.A. Effective minority carrier lifetime and distribution of steady-state excess minority carriers in macroporous silicon. *Chemistry, Physics and Technology of Surface*. 2017. **8**, No. 3. P. 322–332.
4. Onyshchenko V.F., Karachevtseva L.A., Lytvynenko O.O., Plakhotnyuk M.M., Stronska O.Y. Effective lifetime of minority carriers in black silicon nano-textured by cones and pyramids. *Semiconductor Physics, Quantum Electronics & Optoelectronics*. 2017. **20**, No. 3. P. 325–329.
5. Barillaro G., Bruschi P., Pieri F., Strambini L.M. CMOS-compatible fabrication of porous silicon gas sensors and their readout electronics on the same chip. *phys. status solidi* (*a*). 2007. **204**, No. 5. P. 1423–1428.
6. Cardador D., Vega D., Segura T., Trifonov A., Rodríguez A. Enhanced geometries of macroporous silicon photonic crystals for optical gas sensing applications. *Photonics and Nanostructures – Fundamentals and Applications*. 2017. **25**, P. 46–51.
7. Barillaro G., Strambini L.M. An integrated CMOS sensing chip for NO_2 detection. *Sensors and Actuators B*. 2008. **134**, No. 2. P. 585–590.
8. Ernst M., Brendel R., Ferre R. et al. Thin macroporous silicon heterojunction solar cells. *phys. status solidi RRL*. 2012. **6**, No. 5. P. 187–189.
9. Ernst M. and Brendel R. Macroporous silicon solar cells with an epitaxial emitter. *IEEE J. Photovolt*. 2013. **3**, No. 2. P. 723–729.
10. Karachevtseva L., Kartel M., Bo Wang, Sementsov Yu., Trachevskiy V., Lytvynenko O. and Onyshchenko V. "Polymer-multiwall carbon nanotube" nanocoatings on macroporous silicon matrix. *Intern. J. Innovat. Sci., Eng. & Technol*. 2017. **4**, No. 8. P. 93–101.
11. Karachevtseva L.A., Kartel M.T., Konin K.P., Lytvynenko O.O., Onyshchenko V.F., Bo Wang. Light emitting "polymer-nanoparticles" coatings on macroporous silicon substrates. *Chemistry, Physics and Technology of Surface*. 2017. **8**, No. 1. P. 18–29.
12. Karachevtseva L.A., Kartel M.T., Lytvynenko O.O., Onyshchenko V.F., Parshyn K.A., Stronska O.J. Polymer-nanoparticle coatings on macroporous silicon matrix. *Adv. Mater. Lett*. 2017. **8**, No. 4. P. 336–341.
13. Karachevtseva L.A., Lytvynenko O.O., Konin K.P., Parshyn K.A., Sapelnikova O.Yu., Stronska O.J. Electro-optical effects in 2D macroporous silicon structures with nanocoatings. *Semiconductor Physics, Quantum Electronics & Optoelectronics*. 2015. **8**, No. 4. P. 377–384.
14. Onyshchenko V.F. Distribution of non-equilibrium charge carriers in macroporous silicon structure under conditions of their homogeneous generation over the simple bulk. *Optoelectronics and Semiconductor Technique*. 2015. **50**. P. 125–131 (in Ukrainian).
15. Onyshchenko V.F. Distribution of photocarriers in macroporous silicon in case of the spatially inhomogeneous generation of charge-carriers. *Optoelectronics and Semiconductor Technique*. 2016. **51**. P. 158–162 (in Ukrainian).
16. Selj J.H., Marstein E., Thogersen A. et al. Porous silicon multilayer antireflection coating for solar cells; process considerations. *phys. status solidi* (*c*). 2011. **8**, No. 6. P. 1860–1864.
17. Mendoza-Aguero N., Agarwal V., Villafan-Vidales H.I., Campos-Alvarez J. and Sebastian P.J. A heterojunction based on macro-porous silicon and zinc oxide for solar cell application. *J. New Mater. for Electrochem. Systems*. 2015. **18**, No 4. P. 225–230.
18. Treideris M., Bukauskas V., Reza A. et al. Macroporous silicon structures for light harvesting. *Mater. Sci. E*. 2015. **21**, No. 1. P. 3–6.
19. Loget G., Vacher A., Fabre B., Gouttefangeas F., Joanny L. and Dorcet V. Enhancing light trapping of macroporous silicon by alkaline etching: application for the fabrication of black Si nanospike arrays. *Materials Chemistry Frontiers*. 2017. **9**. P. 1881–1887.
20. Karachevtseva L., Glushko O., Karas' M., Onishchenko V. Surface waves in 2D photonic macroporous silicon structures. *Proc. SPIE*. 2005. **5733**. P. 297–307.
21. Karachevtseva L.A., Onyshchenko V.F., Sachenko A.V. Kinetics of photoconductivity in macroporous silicon structures. *Ukr. J. Phys*. 2008. **53**, No. 9. P. 874–881.